Kirkuk Journal of Science Vol. 20, Iss. 3, p. 31-40, 2025 doi:10.32894/kujss.2025.161544.1217

Design the Impact of Temperature on the Modulation Bandwidth of InGaAs vertical cavity surface emitting lasers (VCSELs) for Efficient Optical Interconnect

Abdullah Ibrahim Abdullah *, Faten Adel Ismael Chaqmaqchee

Department of Physics, Faculty of Science and Health, Koya University, Koya 44023, Kurdistan Region – F.R. Iraq
*Corresponding author : abdullaibrahimabdulla83@gmail.com

Article Information

Article Type:
Research Article

Keywords:
VCSEL, high-speed modulation, temperature stability, output power, optical interconnects.

History:
Received: 15 June 2025
Revised: 25 July 2025
Accepted: 26 July 2025
Available Online: 30 September 2025

Citation: Abdullah Ibrahim Abdullah, Faten Adel Ismael Chaqmaqchee, Design the Impact of Temperature on the Modulation Bandwidth of InGaAs vertical cavity surface emitting lasers (VCSELs) for Efficient Optical Interconnect, Kirkuk Journal of Science, 20(3), p. 31-40, 2025, https://doi.org/10.32894/kujss.2025.161544.1217

Abstract

This simulation work, based on the design of an 850 nm InGaAs/AlGaAs quantum well (QWs) vertical cavity surface emitting laser (VCSEL), presents significant challenges, particularly due to the limitations of device bandwidth at higher temperatures. We propose a comprehensive modelling approach to optimize the dynamic performance of a VCSEL structure with an oxide aperture diameter of 6 μm, specifically to achieve higher bandwidth at lower bias currents. The MATLAB simulation evaluates the variation of critical parameters, such as threshold current, differential efficiency, output power, and small-signal modulation, across a wide operating temperature range. Our findings indicate that in static analysis, the threshold current exhibits a positive temperature dependence, increasing with rising temperature, while both differential efficiency and optical output power decrease. Dynamic analysis reveals that although the 3-dB modulation bandwidth reduces with temperature, the VCSEL maintains high-speed performance exceeding 36 GHz at 20 ^{o}C and 24 GHz at 120 ^{o}C under a bias current of 14 mA. The temperature dependence of the modulation current efficiency factor (MCEF) provides insight into optimizing VCSEL structures for reliable high-speed operation over broad thermal conditions.

1. Introduction:

Vertical cavity surface emitting lasers (VCSELs), first proposed by Iga in 1978, have significantly advanced in modern optoelectronic devices [1], [2]. VCSELs serve as a dominant light source in data centers, supercomputers and high-performance computing (HPC) systems owing to their low power consumption, cost efficiency, compact size and ease of integration into large arrays, and they play a critical role in today's short-range optical interconnects [3], [4]. Despite their advantages, the integration of VCSELs into next generation data communication systems is challenged by restricted modulation bandwidth and reduced efficiency under elevated thermal conditions [5]. Among the range of VCSEL emission wavelengths, 850 nm devices are particularly important, making them ideal for short-reach data communication systems [6], [7].

Temperature-related performance of VCSELs is highly dependent on the structural design parameters, including an oxide aperture diameter, mirror reflectivity of the distributed Bragg mirrors (DBRs), and gain-cavity detuning.

3005-4788 (Print), 3005-4796 (Online) Copyright © 2025. This is an open access article distributed under the terms and conditions of the Creative Commons Attribution (CC-BY 4.0) license (https://creativecommons.org/license/by/4.0/)

The use of multi QWs, carefully strain - optimized detuning, are among the strategies identified in previous studies to mitigate this thermal performance degradation [8]. Together, these factors strongly impact device efficiency and operational stability under various temperature conditions [9]. However, VCSELs inherently exhibit temperature sensitivity, with both static and dynamic operational performance as temperature increases. The impact of temperature on device behavior is essential to ensure reliable operation, especially as networks demand higher data rates [10].

In particular, with increasing temperature, the static parameters of the VCSEL - threshold current, output power, and differential efficiency degrade due to increased non-radiative recombination, reduced gain, and thermal rollover [11]. The performance of VCSEL devices is very sensitive to temperature changes. For example, studies have shown that the threshold current of VCSELs can increase by nearly twice its value with increasing temperature from T=20 to 100 ^{o}C, while slope efficiency can decrease by over 40% in this range [12]. Even at T=20 ^{o}C, the output power deviates from the linear trend predicted by simple rate equation modelling, which does not consider thermal effects.

Additionally, the output optical power increases with diameters but increase thermal heating [13]. On the dynamic side, increased operating temperatures cause a shift in the resonant frequency and an increase in damping, thereby reducing the small-signal modulation bandwidth and modulation current efficiency factor (MCEF) [3]. VCSELs at room temperature can achieve a small signal modulation bandwidth of up to ∼28 GHz at optimal biasing conditions. However, this value decreases significantly at higher temperatures unless the drive current is increased or the cavity structure is refined and thermally optimized [5].

This work presents a simulation and analysis of the temperature dependence behavior of 850-nm VCSELs with an oxide aperture diameter of 6 μm in the range of 20-120 ^{o}C. Theoretical frameworks based on carrier and photon dynamics equations, are used together with material parameters from the literature [14] to analyze the optical output power, current-voltage (LIV), and 3dB modulation bandwidth, which vary with temperature. By comparing our simulation results with experimental works, we identify the key design parameters that most strongly impact the thermal stability of 850 nm VCSELs. These findings offer guidance for optimizing device design to ensure reliable high-speed operation in thermally challenging environments of advanced data communication platforms.

2. Device design:

The VCSEL structure was designed for 850 nm emission light using Matlab simulation. The DBR mirrors are made by multiple thin layers with alternating low and high refractive indices. Each layer is a quarter of the target emission wavelength. As shown in Figure 1(a), the top mirror comprise 20-pairs of p-doped layers $Al_{0.9}Ga_{0.1}As$/ $Al_{0.15}Ga_{0.85}As$, while the bottom contains 35-pairs of n- doped layers of same composition. Such a layered design minimizes electrical resistance and also limits optical absorption. Two 30 nm thick $Al_{0.98}$Ga0.02As layers are positioned just before oxidation layers, providing confinement for both carriers and photons.

The 1.5-λ-thick optical cavity employs five strained $In_{0.0-5}Ga_{0.95}As$ QWs, separated by $Al_{0.3}Ga_{0.7}As$ barriers. A GaAs buffer layer of 1.58 μm thickness is placed below n-doped DBRs to ensure mechanical stability. All the expitaxial structures are designed and grown on n+ GaAs substrate. In Figure 1(b) shows the calculation of the reflectance and the quality factor (Q) as a functions of the number of DBR pairs for the same structure design, where the Q-Factor is defined as the ratio of the central wavelength (λ_o) to the linewidth $\triangle\lambda$ [15] of the cavity resonance of VCSEL. For a DBRs with 20-pairs, the highest Q-Factor achieved is approximately 21.3×10^3, with a corresponding reflectivity of 99.5%. Temperature significantly affects nearly all physical processes in semiconductor laser devices, including VCSELs, making it essential to understand how the fundamental parameters change with temperature. Most of the electrical input energy is naturally converted to heat within the laser [16]. To qualitatively assess these thermal effects, the output optical power P_{out} above threshold is calculated by [17]:

$$P_{out} = \eta_d \frac{(h\nu)}{q} e^{\frac{\triangle T_j}{T_i}} (I - I_{th}) \quad (1)$$

where η_d is the differential efficiency, which is modeled to decrease with temperature, $h\upsilon$ is the photon energy at 850 nm, q is the electron charge, I is the injection current and $\triangle T_j$ is the is the junction temperature rise with respect to the heat sink temperature. T_i is a characteristic temperature related to thermal effects [18]. The differential efficiency $\eta_d = \eta_i \alpha_m/\alpha_m + \alpha_i$ depends on the internal quantum efficiency η_i , mirror losses α_m and internal losses α_i as in [11]. The active region temperature rise is calculated $\triangle T_j = R_{th}$ (VI-P_{out}) as in [19], where V is the voltage across the device and IV is the electric input power. These temperature-dependent effects highlight the importance of efficient thermal management and optimized VCSEL design to maintain stable operation across a wide temperature range.

The dynamic performance of 850 nm VCSELs under varying temperature conditions is characterized by the interaction between carriers and photons above the lasing threshold, typically described using rate equations. The S21 can be approximated using a transfer function that models the system as a second-order response with additional parasitic low-pass

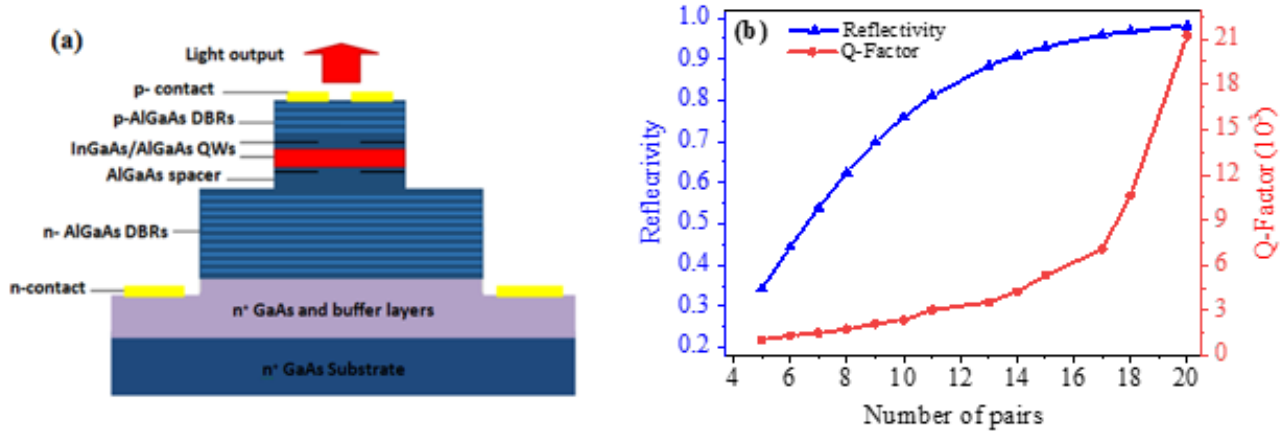

Figure 1. (a) Schematic cross section of VCSEL with 850 nm active medium enclosed between top and bottom DBRs, (b) simulated reflectance (bule) and Q-Factor (red) vesus number of pairs of InGaAs/AlGaAs VCSEL structure.

filtering [20].

$$H(f) = const.\frac{f_r^2}{f_r^2 + f^2 + j(\frac{f}{2\pi})\gamma}.1(1 + j(\frac{f}{f_p})) \quad (2)$$

where, f_r is the resonance frequency, Υ is the damping factor, and f_p denotes the parasitic cut-off frequency, which arises due to RC limitations in the device. At low temperatures of 20 ^{o}C, this transfer function exhibits a pronounced resonance peak at lower bias currents due to reduced differential gain and gain detuning, resulting in a lower f_r. The pronounced resonance peak refers to a sharp peak in the small-signal modulation response S21, which appears under certain bias and temperature conditions.

Physically, it reflects a strong relaxation oscillation due to efficient carrier-photon interactions in the VCSEL cavity. At lower temperatures and low bias currents, the differential gain is higher and the damping is lower, resulting in an underdamped system with a strong resonant enhancement. This peak diminishes as the temperature increases due to enhanced damping, which flattens the modulation response. As the temperature increases, f_r increases while the threshold current I_th decreases, which collectively enhance damping and lead to a more uniform and less peaked frequency response, The resonance frequency f_r is related to the bias current I by [21], [22]:

$$f_r = D.\sqrt{I - I_{th}} \quad (3)$$

$$D = \frac{1}{2\pi}.\sqrt{\frac{\eta_i \Gamma \upsilon_g}{q\upsilon_a}.\frac{\partial g/\partial n}{\chi}} \quad (4)$$

where Γ is the optical confinement factor, v_g is the group velocity, q the elementary charge, v_a the active region volume, $\partial g/\partial n$ the differential gain, and χ is the transport factor. The D-factor (or modulation current efficiency factor (MCEF)) is the relation between f_r and $\sqrt{I - I_{th}}$. Large D- factors are generally preferred for the high-speed operation of VCSEL device [23].

This value is among the best reported to date, which is credited to a smaller cavity size. The damping factor Y determines how quickly the resonance decays, following a quadratic dependence on the resonance frequency [24]. The measured modulation response is often plotted in decibels to reflect the logarithmic nature of signal attenuation and gain [25].

3. Result and Discussion

In support of the above discussions, we carried out detailed temperature-dependent electrical characterization of VCSEL devices [26], [27]. Figure 2 shows the static characteristics of an oxide-confined 850 nm QWs VCSEL with a 6 μm aperture diameter measured over temperatures ranging from 20 to 100 ^{o}C. The light output power and voltage versus current (LIV) characteristics illustrate the typical device behavior with increasing current and temperature (Figure 2a).

As the temperature rises, the threshold current shifts higher and the output power decreases, which is clearly visible in these curves. The extracted maximum differential efficiency and threshold current as functions of temperature reveal a steady decline in differential efficiency from 0.9 W/A at 20 ^{o}C to 0.67 W/A at 100 ^{o}C, while the threshold current nearly doubles from 0.28 mA to 0.57 mA over the same range (Figure 2b).

The maximum output power similarly decreases with temperature, dropping from approximately 8.3 mW at 20 ^{o}C to 5.7 mW at 100 ^{o}C, and the power conversion efficiency falls

from around 83% to 55% (Figure 2c). Finally, the threshold current and current density both increase with temperature, indicating higher carrier losses and reduced gain efficiency at elevated temperatures; threshold current density rises from about 1.1 kA/cm^2 to 2.3 kA/cm^2 between 20 and 100 ^{o}C (Figure 2d). These trends are consistent with expected thermal effects in semiconductor lasers, highlighting the need for effective thermal management to maintain optimal device performance. Figure 3 presents the simulated small-signal modulation response (S21 in dB) of an InGaAs VCSEL with a 6 μm aperture diameter, evaluated across a temperature range from T=20 to 120 ^{o}C and bias currents between 2 and 14 mA. The simulations extend up to 40 GHz to capture the device's high-frequency behavior. At T=20 ^{o}C, the VCSEL achieves a maximum 3 dB modulation bandwidth approaching 36 GHz for bias currents between 10 and 14 mA. As the temperature increases, the modulation bandwidth gradually decreases due to enhanced thermal effects impacting carrier dynamics and material properties.

At T=40 and 60 ^{o}C, the 3- dB bandwidth moderately decreases to approximately 32–34 GHz and 28–30 GHz, respectively, within the same current range. At 80 ^{o}C, the bandwidth further reduces to about 27–30 GHz, reflecting typical thermal roll-off behavior inherent in VCSEL devices. Even at elevated T= 100 and 120 ^{o}C, the device maintains a 3 dB bandwidth above 24 GHz for bias currents between T=10 and 14 mA, indicating strong temperature stability suitable for high-speed operation.

The simulation results consistently show that increasing bias current enhances modulation bandwidth at each temperature, attributed to the rise in resonance frequency. However, the bandwidth improvement saturates beyond approximately 12 mA due to the onset of nonlinear effects and thermal limitations. These findings highlight the robust high-speed performance of the 6 μm aperture VCSEL across a broad temperature range, affirming its suitability for practical optical communication systems requiring stable and reliable operation under varying thermal conditions.

Table 1 presents a comparative analysis between the simulation results of an 850 nm oxide-confined VCSEL (this work) and experimental results reported in recent Multidisciplinary Digital Publishing Institute (MDPI) studies. This comparison serves to validate the predictive accuracy of the simulation model by benchmarking it against established experimental outcomes. Figure 4 illustrates the extracted 3 dB modulation bandwidth (f_{3dB}) of the VCSEL as a function of the square root of the bias current above threshold ($I-I_{th})^{\frac{1}{2}}$, for various ambient temperatures ranging from T=20 to 100 ^{o}C.

The linear fitting of the data confirms the square root dependence of the modulation bandwidth on current above threshold. The simulation is based on threshold currents I_{th} of 295 μA, 345 μA, 400 μA, 470 μA, and 575 μA for 20 ^{o}C, 40 ^{o}C, 60 ^{o}C, 80 ^{o}C, and 100 ^{o}C, respectively. Corresponding MCEF values extracted from the linear slopes are 8.11, 7.78, 7.34, 7.00, and 6.56 GHz/ mA $^{\frac{1}{2}}$, respectively. These results indicate a gradual decline in MCEF with increasing temperature, attributed to thermally induced degradation in differential gain and carrier-photon dynamics. The highest modulation bandwidth is achieved at T=20 ^{o}C and decreases with temperature, consistent with the thermal sensitivity of VCSEL performance. Nevertheless, the near-linear trend and relatively high MCEF values even at T=100 ^{o}C highlight the device's robustness and suitability for high-speed optical interconnects under elevated thermal conditions. Figure 5 shows the normalized D-Factor as a function of temperature for various bias currents ranging from 2 mA to 14 mA. It is clear from this figure that D-factor decreases linearly with increasing temperature and become more damped, leading to slower modulation response. At 2 mA, the D-factor starts lower and decrease more steeply, suggesting that low bias current leads to poor high frequency performance, especially at higher temperature. At higher bias currents from 10 to 14 mA, the damping factor remains higher across the temperature range. This implies better thermal stability and performance at high currents. This behavior shows the effect of temperature on modulation performance and confirms that the VCSELs is sensitive to thermal effects.

4. Conclusion:

In summary, we proposed modeling and simulation of the impact of temperature on 850 nm InGaAs/AlGaAs QWs VCSEL as efficient optical sources within short-reach distance optical interconnects. The device performance demonstrates that despite the degradation in modulation bandwidth at increased temperature, the device maintains high-speed operation with a 3-dB bandwidth of 36 GHz at 20 ^{o}C under bias current of 14 mA and confirming thermal stability up to 120 ^{o}C. Furthermore, by analyzing the MCEF behavior at various temperatures, we identify strategies to improve the thermal performance of VCSELs. This optimized design exhibits strong applicability in thermally demanding applications such as data centers and next generation photonic interconnects. These results strongly support the suitability of the proposed VCSEL structure for advanced practical applications. It's demonstrated thermal resilience and high-speed modulation performance-maintaining over 24 GHz bandwidth even at 120 ^{o}C-make it highly relevant for integration into modern data centers, photonic integrated circuits (PICs), and artificial intelligence (AI) interconnect systems. The Consistent performance over a wide temperature range ensures reliable operation in high-performance environments where thermal control is difficult. As data-driven technology continues to evolve, this design offers a promising solution for high-speed, low-power optical links, making them an essential component of next-generation optical communication infrastructures.

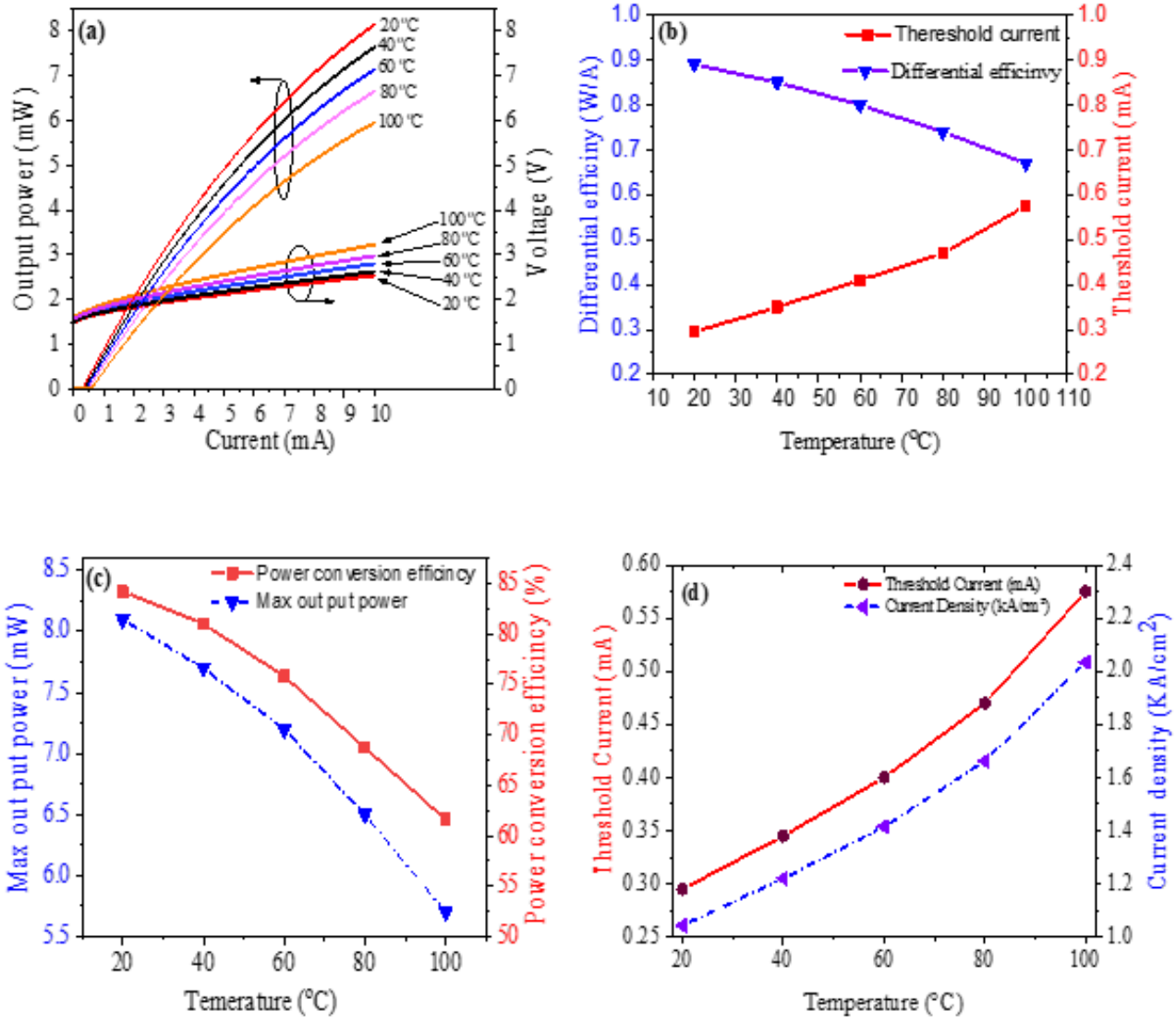

Figure 2. LIV characteristics for the VCSEL with 6 μm aperture (a) and extracted values of the maximum differential efficiency and threshold current (b), maximum output power and power conversion efficiency (c), as well as threshold current and current density (d) at different temperatures between 20 and 100 ^{o}C.

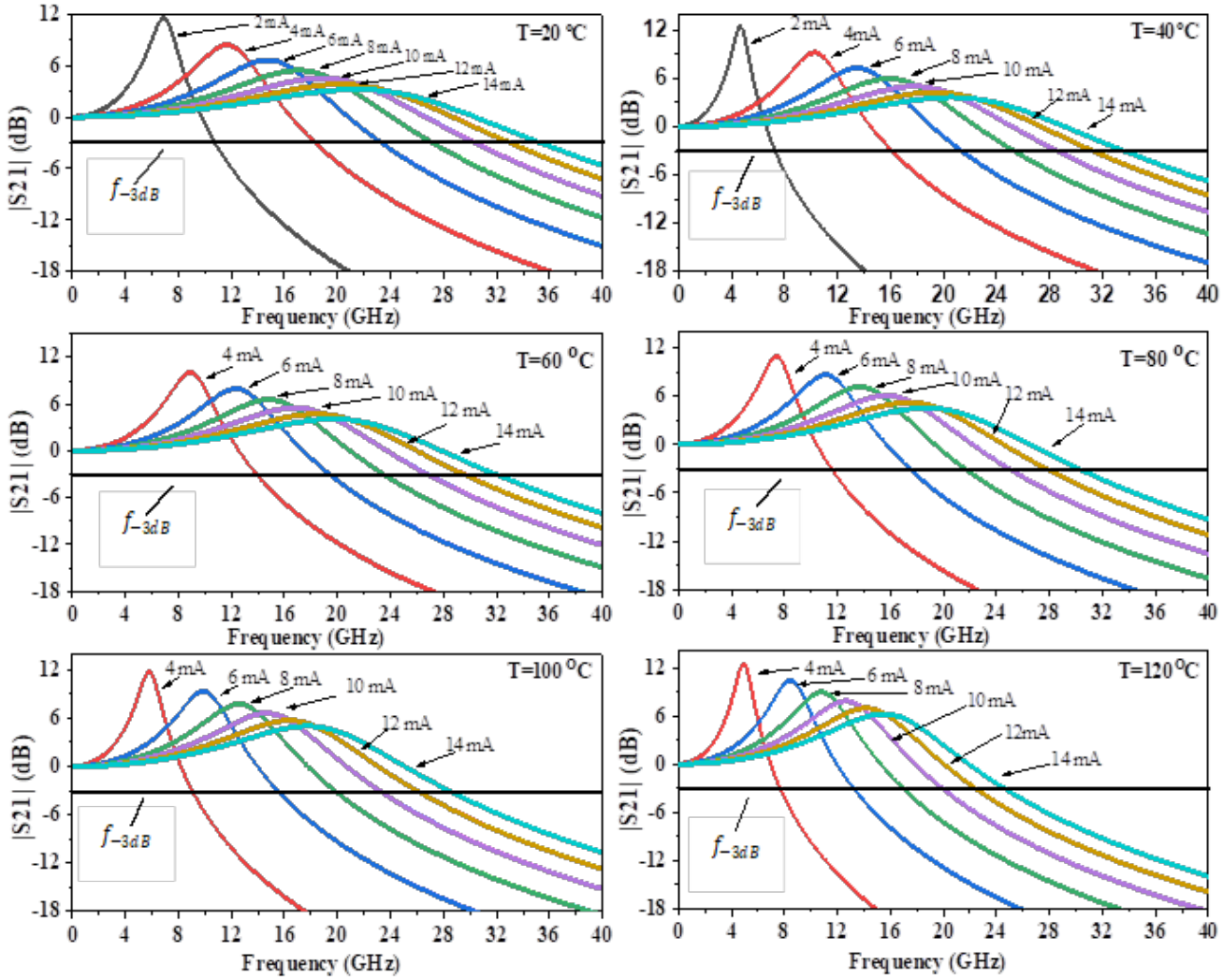

Figure 3. Simulated S21 versus frequency at bias current from 4 to 14 mA and T=20 to 120 ^{o}C.

Table 1. Temperature-dependent efficiency and performance of 850 nm VCSELs: Comparative analysis of simulated and Measured Data.

Study	Operating Temperature (^{o}C)	Threshold Current (mA)	Optical Power (mW)	Differential Efficiency (W/A)	MCEF (GHz/mA∧0.5)	Bandwidth (GHz)
This Work (simulated)	20–120	0.28–0.57	5.6–8.2	0.65–0.89	8.11–6.56	36–26
Cheng et al. [3]	25–85	1.5–4.1	1.8–5.5	0.20–0.35	5.12–3.21	20–15
Mutig. [12]	25–85	0.6–2.8	2.4–5.0	0.25–0.45	4.3–2.5	18–12
Du et al. [4]	25–85	1.55–3.70	12.62–3.5	0.30–0.45	6.19–4.41	18.5–11.9
Aziz et al. [14]	25–140	6–18.5	0.8–13.2	0.72–0.84	Not Reported	32–11.5 / 20.3–14.1
Westberg et al. [28]	25–85	0.83–1.37	4.9–9.4	0.62–0.75	Not Reported	28–21 / 27–21
Aziz (2024) – Thesis. [29]	25–140	1.1–18.5	2.7–13.2	0.62–0.84	Not Reported	32 (RT), 14 (140 ^{o}C)

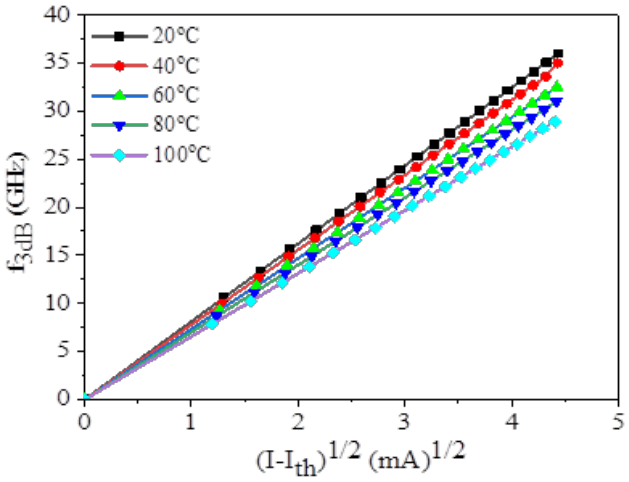

Figure 4. f_{3dB} of the VCSEL as a function of the square root of the bias current above the threshold at different term.

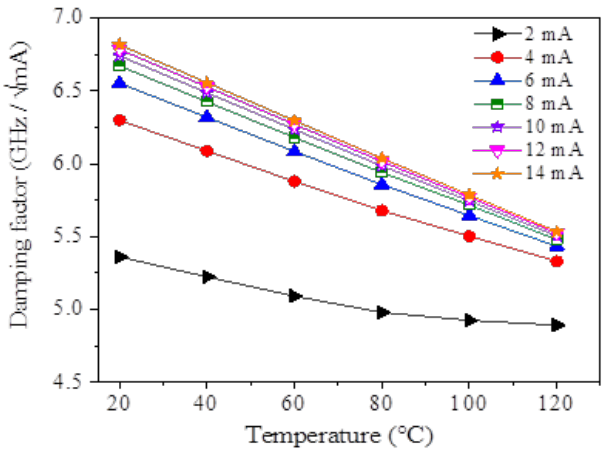

Figure 5. Normalized damping factor ($\Upsilon/\sqrt{I}$) vs. temperature at various bias currents.

Funding: None.

Data Availability Statement: All of the data supporting the findings of the presented study are available from corresponding author on request.

Declarations:
Conflict of interest: The authors declare that they have no conflict of interest.

Ethical approval: The study was carried out using MATLAB for simulations and computational analysis. Since no human subjects or animals were involved, ethical approval was not necessary.

Author Contributions: This research was carried out as part of the MSc work in the department of physics, faculty of science and health, Koya University. The author would like to express his sincere appreciation for the support and guidance provided by her superviour and colleagues throghout this research.

References

[1] K. Iga. Vertical-cavity surface-emitting laser: Its conception and evolution. *Japanese Journal of Applied Physics*, 47(1): 1, 2008, doi:10.1143/jjap.47.1.

[2] B. Weigl et al. High-performance oxide-confined gaas vcsels. *IEEE Journal of Selected Topics in Quantum Electronics*, 3(2): 409–415, 1997, doi:10.1109/2944.605686.

[3] H.-T. Cheng, Y.-C. Yang, T.-H. Liu, and C.-H. Wu. Recent advances in 850 nm vcsels for high-speed interconnects. *in Photonics*, 9(2): 107, 2022, doi:10.3390/photonics9020107.

[4] F. Adel Ismael Chaqmaqchee and J. A. Lott. Impact of oxide aperture diameter on optical output power, spectral emission, and bandwidth for 980 nm vcsels. *OSA Continuum*, 3(9): 2602–2613, 2020, doi:10.1364/OSAC.397687.

[5] D. M. Kuchta et al. A 50 gb/s nrz modulated 850 nm vcsel transmitter operating error free to 90 c. *Journal of Lightwave technology*, 33(4): 802–810, 2014, doi:10.1109/JLT.2014.2363848.

[6] P. Westbergh et al. High-speed oxide confined 850-nm vcsels operating error-free at 40 gb/s up to 85°c. *IEEE Photonics Technology Letters*, 25(8): 768–771, 2013, doi:10.1109/LPT.2013.2250946.

[7] S. Du et al. Temperature-dependent characteristics of the high-speed 850nm vcsel. *in International Conference on Optoelectronic Information and Functional Materials*, 13183: 56–61, 2024, doi:10.1117/12.3033973.

[8] H. D. Kaimre, A. Grabowski, J. Gustavsson, and A. Larsson. Effects of detuning on wide-temperature behavior of 25 gbaud 850nm vcsels. *in Vertical-Cavity Surface-Emitting Lasers XXVII*, 12439: 92–104, 2016, doi:10.1117/12.2648918.

[9] M. Feng, C.-H. Wu, and N. Holonyak. Oxide-confined vcsels for high-speed optical interconnects. *IEEE Journal of Quantum Electronics*, 54(3): 1–15, 2018, doi:10.1109/JQE.2018.2817068.

[10] R. Michalzik and K. J. Ebeling. Operating principles of vcsels. *in Vertical-Cavity Surface-Emitting Laser Devices: Springer*, 953-98, 2003, doi:10.1007/978-3-662-05263-1_3.

[11] F. A. I. Chaqmaqchee. Fabrication and characterization of stable temperature and reliable size oxide aperture vcsels for short-reach communication. *Journal of Optics*, 53(4): 3453–3462, 2023, doi:10.1007/s12596-023-01519-w.

[12] A. Mutig. *High speed VCSELs for optical interconnects*. Springer Science Business Media, 2011.

[13] P. P. Baveja et al. Assessment of vcsel thermal rollover mechanisms from measurements and empirical modeling. *Optics express*, 19(16): 15490–15505, 2011, doi:10.1364/OE.19.015490.

[14] M. B. Aziz, H. D. Kaimre, and A. Peter. High-speed transmission of 850 nm vcsel optical interconnects across wide temperatures. *IEEE Photoics Technology Letters*, 1, 2024.

[15] T. Rogers, D. Deppe, and B. Streetman. Effect of an alas/gaas mirror on the spontaneous emission of an ingaas-gaas quantum well. *Applied physics letters*, 57(18), 1990, doi:10.1063/1.104120.

[16] L. Mawst, N. Tansu, and A. Rahman. Quantum-well lasers and their applications. *Reference Module in Materials Science and Materials Engineering*, 18(2): 1–51, 2011, doi:10.1016/B978-0-12-803581-8.00825-0.

[17] P. Blood, S. Colak, and A. Kucharska. Temperature dependence of threshold current in gaas/algaas quantum well lasers. *Applied physics letters*, 52(8): 599–601, 1988, doi:10.1063/1.99647.

[18] P. Westbergh, R. Safaisini, E. Haglund, J. S. Gustavsson, A. Larsson, and A. Joel. High-speed 850-nm vcsels with 28 ghz modulation bandwidth for short reach communication. *in Vertical-Cavity Surface-Emitting Lasers XVII*, 8639: 251–256, 2013, doi:10.1117/12.2001497.

[19] M. Daubenschüz and R. Michalzik. Parameter extraction from temperature-dependent light-current-voltage data of vertical-cavity surface-emitting lasers. *in Semiconductor Lasers and Laser Dynamics VII*, 9892: 115–122, 2016, doi:10.1117/12.2228080.

[20] O. Kjebon, R. Schatz, S. Lourdudoss, S. Nilsson, and B. Stalnacke. Modulation response measurements and evaluation of mqw ingaasp lasers of various designs. *in High-Speed Semiconductor Laser Sources*, 2684: 138–152, 1996, doi:10.1117/12.236941.

[21] L. A. Coldren, S. W. Corzine, and M. L. Mashanovitch. *Diode lasers and photonic integrated circuits*. John Wiley Sons, 2012.

[22] P. Westbergh, J. S. Gustavsson, Å. Haglund, M. Skold, A. Joel, and A. Larsson. High-speed, low-current-density 850 nm vcsels. *IEEE Journal of Selected Topics in Quantum Electronics*, 15(3): 694–703, 2009, doi:10.1109/JSTQE.2009.2015465.

[23] Y.-C. Yang, H.-T. Cheng, and C.-H. Wu. 30 ghz highly damped oxide confined vertical-cavity surface-emitting laser. *in 2021 IEEE Photonics Conference*, 1-2, 2021, doi:10.1109/IPC48725.2021.9592916.

[24] M. Gebski, P.-S. Wong, M. Riaziat, and J. A. Lott. 30 ghz bandwidth temperature stable 980 nm vertical-cavity surface-emitting lasers with alas/gaas bottom distributed bragg reflectors for optical data communication. *Journal of Physics: Photonics*, 2(3): 035008, 2020, doi:10.1088/2515-7647/ab9420.

[25] G. Larisch, S. Tian, and D. Bimberg. Optimization of vcsel photon lifetime for minimum energy consumption at varying bit rates. *Optics Express*, 28(13), 2020, doi:10.1364/OE.391781.

[26] H. D. Kaimre, A. Grabowski, J. Gustavsson, and A. Larsson. 25 gbaud 850 nm vcsel for an extended temperature range. *IEEE Photonics Technology Letters*, 2025, doi:10.1109/LPT.2025.3547156.

[27] A. Mutig et al. Frequency response of large aperture oxide-confined 850 nm vertical cavity surface emitting lasers. *Applied Physics Letters*, 95(13), 2009, doi:10.1063/1.3231446.

[28] P. Westbergh et al. High-speed 850 nm vcsels with 28 ghz modulation bandwidth operating error-free up to 44 gbit/s. *Electronics Letters*, 48(18): 1145–1147, 2012, doi:10.1049/el.2012.2525.

[29] M. B. Aziz. High-speed optical interconnects in harsh environments. *Chalmers Tekniska Hogskola (Sweden)*, 2024.

تصميم تأثير درجة الحرارة على عرض نطاق التضمين لليزرات الباعثة من السطح للتوصيل البصري *InGaAs* المصنوعة من (*VCSELs*) ذات التجاويف الرأسية الفعال

عبدالله إبراهيم عبدالله * ، فاتن عادل إسماعيل جقملقي

قسم الفيزياء ،كلية العلوم والصحة، جامعة كوية، كوية، اربيل، العراق.

* الباحث المسؤول: *abdullaibrahimabdulla83@gmail.com*

الخلاصة

يعرض هذا العمل المحاكاتي، المبني على تصميم ليزر انبعاث سطحي عمودي (*VCSEL*) بطول موجي 850 نانومتر باستخدام آبار كمومية من نوع *InGaAs/AlGaAs* ، تحديات كبيرة، وخصوصًا بسبب القيود المفروضة على عرض النطاق الترددي للجهاز عند درجات الحرارة المرتفعة. نقترح نهج نمذجة شامل لتحسين الأداء الديناميكي لبنية *VCSEL* بفتحة أكسيدية بقطر 6 ميكرومتر، بهدف تحقيق عرض نطاق ترددي أعلى عند تيارات انحياز أقل. تقوم محاكاة *MATLAB* بتقييم تغير المعلمات الحرجة مثل تيار العتبة، الكفاءة التفاضلية، القدرة الخارجة، والتعديل بالإشارة الصغيرة عبر نطاق واسع من درجات حرارة التشغيل. تشير نتائجنا إلى أنه في التحليل الساكن، يُظهر تيار العتبة اعتمادًا إيجابيًا على درجة الحرارة، حيث يزداد مع ارتفاعها، بينما تنخفض كل من الكفاءة التفاضلية والقدرة البصرية الخارجة. ويُظهر التحليل الديناميكي أنه بالرغم من أن عرض نطاق تعديل 3 ديسيبل ينخفض مع ارتفاع درجة الحرارة، إلا أن طثصيى يحافظ على أداء عالي السرعة يتجاوز 36 ميغاهرتز عند 20 درجة مئوية و 24 ميغاهرتز عند 120 درجة مئوية تحت تيار انحياز قدره 14 مللي أمبير .يعطي الاعتماد الحراري لعامل كفاءة تيار التعديل (*MCEF*) فهمًا أعمق لتحسين هياكل *VCSEL* من أجل تشغيل عالي السرعة وموثوق به ضمن ظروف حرارية واسعة.

الكلمات الدالة : *VCSEL* ، التعديل عالي السرعة، استقرار درجة الحرارة، طاقة الخرج، الترابطات البصرية.

التمويل: لايوجد.

بيان توفر البيانات: جميع البيانات الداعمة لنتائج الدراسة المقدمة يمكن طلبها من المؤلف المسؤول.

اقرارات:

تضارب المصالح: يقر المؤلفون أنه ليس لديهم تضارب في المصالح.

الموافقة الأخلاقية: تم إجراء الدراسة باستخدام برنامج *MATLAB* لأغراض المحاكاة والتحليل الحاسوبي. ونظرًا لعدم إشراك أي أشخاص أو حيوانات في الدراسة، لم تكن هناك حاجة للحصول على موافقة أخلاقية.

مساهمات المؤلفين: أُجري هذا البحث كجزء من دراسة الماجستير في قسم الفيزياء، كلية العلوم والصحة، جامعة كويه. وتتقدم الباحثة بخالص الشكر والتقدير للدعم والتوجيه الذي قدمه لها مشرفها وزملاؤها طوال فترة هذا البحث.